On the hybridization isotherms of DNA microarrays: the Langmuir model and its extensions

2006 J. Phys.: Condens. Matter 18 S463

(http://iopscience.iop.org/0953-8984/18/18/S01)

INSTITUTE OF PHYSICS PUBLISHING JOURNAL OF PHYSICS: CONDENSED MATTER

J. Phys.: Condens. Matter **18** (2006) S463–S490 doi:10.1088/0953-8984/18/18/S01

TOPICAL REVIEW

On the hybridization isotherms of DNA microarrays: the Langmuir model and its extensions

A Halperin[1], **A Buhot**[1] **and E B Zhulina**[2]

[1] Structures et Propriétés d'Architectures Moléculaires, UMR 5819 (CEA, CNRS, UJF), DRFMC/SPrAM, CEA-Grenoble, 38054 Grenoble cedex 9, France
[2] Institute of Macromolecular Compounds of the Russian Academy of Sciences, 199004 St Petersburg, Bolshoy prospect 31, Russia

Received 29 July 2005
Published 19 April 2006
Online at stacks.iop.org/JPhysCM/18/S463

Abstract

The design of DNA chip experiments utilizes hybridization isotherms relating the equilibrium hybridization at the surface to the composition of the solution. Within this family, the Langmuir isotherm is the simplest and the most frequently used. This tutorial review summarizes the domain of validity of the Langmuir isotherm and discusses the modifications necessary to allow for competitive hybridization in the bulk and at the surface, probe polydispersity and interactions between the probe sites. The equilibrium constant of hybridization at an impenetrable surface is described, as well as the relative merits of the melting temperature and c_{50} as design parameters. The relevance to various experimental situations, including two-colour experiments, study of point mutations for cancer diagnostics, genotyping of pooled samples and aspects of Latin square experiments, is discussed.

(Some figures in this article are in colour only in the electronic version)

Contents

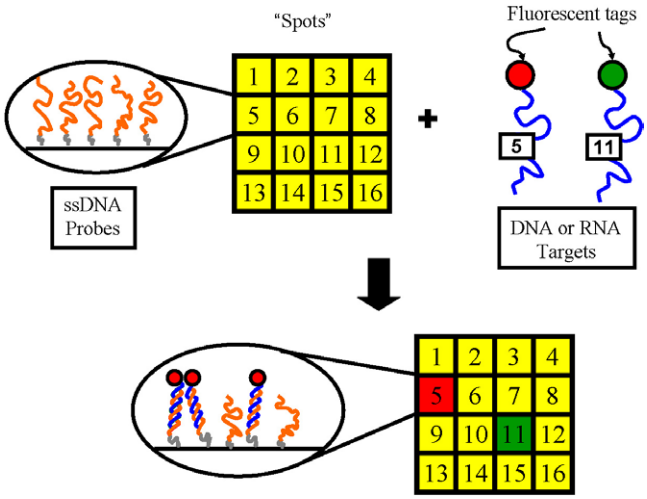

Figure 1. A schematic picture of a DNA chip before and after hybridization with a binary solution of two labelled targets, complementing the probes on spots 5 and 11.

1. Introduction

DNA microarrays, 'DNA chips', are analytical devices designed to determine the composition of multicomponent solutions of nucleic acids (NA), DNA or RNA [1–6]. In its current form, this technology is motivated by the outcome of the Human Genome Project as illustrated by two numbers: the human genome consists of approximately 30 000 genes; the number of single-nucleotide polymorphisms (SNP) is estimated at three million. Two major challenges emerge. One concerns gene expression. The number and identity of the active genes vary with the state and identity of the cell. The challenge is thus to correlate the gene expression profiles, as revealed by the concentrations of the different messenger RNA molecules, with the cell type, its state etc. The second challenge is to understand the role of SNPs—for example, correlate SNPs with propensity to disease. In this type of experiment the primary analyte is the genomic DNA. Sequential analysis of the composition of such multicomponent NA samples, with these numbers in mind, is enormously time-consuming. The desired alternative is a parallel method of analysis designed to simultaneously determine the concentration of the different NA sequences in the interrogated solution. Currently, DNA microarray technology is the leading contender for this role on a genome scale. DNA chips function by simultaneous hybridization of labelled NA sequences in the solution, known as targets, to an array of DNA probes bound to a surface. Numerous identical probes are localized at a small area known as a 'spot' or 'probe cell'. Each probe hybridizes preferentially with targets incorporating a complementary base sequence. The composition of the sample is then deduced from the label intensities of the different spots after the hybridization (figure 1).

Since the current concept of DNA chips emerged in 1996[3], the number of publications in this area has reached the thousands and a number of industrial companies produce DNA microarrays. The physical chemistry of these devices, experiment and theory, lags behind and the number of publications in this area is minuscule in comparison [10]. The rapid development of this technology and its growing popularity gave rise to concerns about standardization in

[3] 1996 was cited as the year for the achievement of DNA microarrays as a genome scale technology for functional analysis [7]. A historical perspective from the point of view of key patents is provided in [8, 9].

manufacturing DNA chips, experimental protocols, the format for reporting results of DNA microarray experiments and the analysis of the data [11]. Of particular note are studies reporting poor concordance between experiments utilizing identical samples but DNA chips produced by different methods [12–14]. Two questions are involved. First, is the composition of the solution hybridized with the DNA chip simply related to that of the initial biological sample? The transformation of the biological sample into a hybridization solution is a multistep process involving extraction, purification, amplification and labelling. In turn, each step can introduce artefacts. This issue is beyond the scope of this review. It focuses instead on the second key question: how does one relate the composition of the solution to the intensities of the spots? A better understanding of the physical chemistry of DNA chips can shed light on the second question and thus contribute to experimental design and the quantification of the results.

This short review concerns theoretical issues associated with the function and design of DNA chips. Since it is intended to be didactic in style, a narrower focus is needed. To this end we first distinguish between two leading formats of DNA chips. In cDNA microarrays, long cDNA[4] targets are physisorbed onto the substrate, while in oligonucleotide chips short oligonucleotide targets are chemically bound to the surface via their terminal groups. Of these, the second format is more amenable to physical chemistry studies because it avoids complications associated with the configurations of the physisorbed cDNA probes and their lability. Accordingly, we limit the discussion to oligonucleotide chips. Theory efforts in this last domain developed in two complementary directions motivated by different types of experiment. One direction is the analysis of the Latin square calibration experiments reported by Affymetrix [16]. In these, samples containing a complex 'background' RNA are spiked with a number of different transcripts at a systematically varied set of concentrations in the pM range. These samples are then hybridized with the Affymetrix high density chip corresponding to the organism in question. The second course is motivated by 'physical chemistry' experiments using self-made oligonucleotide arrays involving a single probe–target pair with no background [17–21]. In this group, the parameters varied include the density of probes at the surface, the number of bases in the target and the hybridization time. In contrast, these parameters are held constant in the Latin square experiments. In the following we focus on the theory directed towards the 'physical chemistry' experiments while commenting occasionally on results concerning the Latin square data. Within the 'physical chemistry' domain it is further possible to distinguish between two directions concerned respectively with the temporal development of the hybridization and the characterization of the final equilibrium states. This review is mostly aimed at the equilibrium behaviour that sets bounds on the performance of DNA chips. In particular, we will discuss the hybridization isotherms of DNA microarray that relate the equilibrium fraction of hybridized probes, x_{eq}, to the composition of the solution. The simplest hybridization isotherm, and the one most widely used, is the Langmuir isotherm, $x_{\mathrm{eq}}/(1-x_{\mathrm{eq}}) = Kc_t$. Here c_t is the concentration of the target interrogated and K is the corresponding equilibrium constant. It has been used to analyse experimental data [18–20, 22–27] and in the formulation of model based algorithms [28, 29]. Explicitly or implicitly it provides a starting point for the development of theoretical models of DNA chips [30–40]. Similarly, it also serves as a basis for the current use of melting temperatures of the hybridized probes as a criterion for probe design [41]. The Langmuir isotherm is however the outcome of a highly idealized model, reminiscent in role and limitations of the

[4] cDNA, complementary DNA, is a term for DNA copies of messenger RNA (mRNA) produced by use of the enzyme reverse transcriptase. The outcome of this reaction is double-stranded RNA–DNA. Single-stranded cDNA is obtained by alkali degradation of the RNA. The single-stranded cDNA can be converted into a double-stranded form by use of DNA polymerase [15].

ideal gas. When invoking the Langmuir isotherm it is important to note these limitations. It is also necessary to extend the model so as to allow for important factors that are not built into it. Our discussion concerns three principal issues. The first is the relationship between the hybridization equilibrium constants at the surface and in the bulk, in particular the modifications of K when the hybridization takes place at an impenetrable surface. The second is the effect of competitive hybridization reactions, at the surface and in the bulk. Finally we consider the consequences of interactions between the probe sites. We initially examine the first two issues for the interaction free case and then consider the effect of interactions when no competitive hybridization reactions take place. Prior to the discussion of these issues we introduce the Langmuir isotherm in the context of DNA chips. In particular, we focus on the utility of c_{50}, the target concentration corresponding to 50% hybridization at the surface, as a measure of sensitivity and a guide for probe design.

Before we proceed, it is useful to summarize the relevant characteristics of DNA microarray experiments. Three parameters play a key role in our discussion: the number of bases in the target, N_t, and in the probe, n, as well as the surface area per probe, Σ_0. Typical values of n lie in the range 10–60. Reported values of the average probe density within a spot vary between 1.2×10^{10} and 4×10^{13} probes cm^{-2} corresponding to 2.5×10^2 Å^2 $\leqslant \Sigma_0 \leqslant$ 8.3×10^5 Å^2. It is important to note that *in situ* synthesis of the probes by means of photolithography or inkjet technology gives rise to polydispersity in n. This problem is not an important factor when the presynthesized probes are used. The polydispersity of Σ_0 is not well characterized but may be of importance. The range of N_t for DNA samples depends on the choice of primers used for the polymerase chain reaction (PCR) [15] amplification or on the fragmentation step in the sample preparation. PCR products are monodispersed while fragmentation introduces polydispersity. Only the average N_t is controlled when fragmentation is used. Typical N_t values for PCR samples are in the range of $100 \leqslant N_t \leqslant 350$ while for fragmented samples the reported values of the average N_t are in the $50 \leqslant N_t \leqslant 200$ range. Besides N_t, n and Σ_0, it is important to note the role of two additional aspects of the chip design. One concerns the surface treatment. In particular, was the surface treated so as to repress non-specific adsorption of NA? The second concerns the grafting chemistry: was the probe anchored to the surface directly or via a spacer chain? In the following we will focus on systems with passivated surfaces and probes bound to the surface via short flexible spacers that weaken the steric constraints to hybridization. With regard to the sample characteristics it is useful to note the role of additional factors. First, labelling the targets can affect the hybridization behaviour. This is mostly a problem with bulky fluorescent tags [42] and it is not an issue with radioactive labels or with label free measurements. In the following we assume ideal labels having no effect on the hybridization. Second, it is important to distinguish between RNA and DNA targets because of differences among the free energies of hybridization and the RNA propensity for forming secondary structures such as hairpins. Our discussion of the hybridization isotherms focuses on the simplest case: DNA oligonucleotide chips interacting with DNA targets. The general features of our analysis also apply to chips hybridizing with RNA targets. However, a detailed analysis of this case should allow for the role of the secondary structure of RNA and its modification by the labels. Third, it is important to distinguish among DNA samples: between the ones comprising double-stranded (dsDNA) and those of single-stranded DNA (ssDNA). Samples of dsDNA targets undergo intermolecular competitive hybridization in the bulk in contrast to those of ssDNA. It is useful to stress again the differences between bioanalytical and physical chemistry experiments. The Latin square experiments, like all bioanalytical experiments, involve a multicomponent solution. In physical chemistry experiments single-component solutions are possible and the concentrations of all components are known. Importantly, the

number of components determines the role of competitive hybridization reactions. Clearly, competitive hybridization is minimal in single-component solutions when self-hybridization is the only competitive reaction possible. Another difference between the two concerns N_t. In biology experiments $N_t \gg n$, while in physical chemistry and calibration experiments the $N_t = n$ option is encountered. Apart from the characteristics of the chip and the sample it is necessary to comment on the hybridization conditions. Two parameters, the hybridization time and hybridization temperature, are especially relevant. Typical values for the first vary between 2 and 12 h. Such hybridization times may be insufficient for equilibration. The hybridization temperature is usually in the range of 30–60 °C. The hybridization temperature is chosen to be lower than the melting temperature of the hybridized probes so as to favour the ds form. It should not be too low in order to avoid excessive non-specific hybridization. Finally, the hybridization is normally carried out at high ionic strength in solutions containing 1 M of NaCl. This last point is important, as we shall discuss, because of the consequent strong screening of the electrostatic interactions.

2. The Langmuir isotherm

The Langmuir isotherm is the starting point for the analysis of the equilibrium behaviour of DNA chips. To introduce it, in this context, consider the hybridization between two species, a probe p immobilized at the surface and a free single-stranded target in the solution, t. The Langmuir isotherm for the hybridization reaction $p + t \rightleftharpoons pt$ is

$$\frac{x_{\mathrm{eq}}}{1 - x_{\mathrm{eq}}} = c_t K_{pt}. \tag{1}$$

Here x_{eq} is the equilibrium fraction of hybridized probes, c_t is the initial concentration of the target and K_{pt} is the equilibrium constant for the hybridization reaction at the surface. In view of our subsequent discussion note that K_{pt} is independent of x_{eq}. This form applies to the small spot limit, where the hybridization at the surface does not affect c_t. In the simplest case x_{eq} is proportional to the spot intensity I and

$$x_{\mathrm{eq}} = \frac{I}{I_{\mathrm{max}}}. \tag{2}$$

I_{max}, the maximal intensity of the spot at saturation, is proportional to the number of probes within it. It is important to note that I_{max} typically varies from spot to spot because of imperfect control of the number of probes per spot. Depending on the labelling and detection scheme I_{max} can also vary with the temperature.

When is the Langmuir isotherm applicable? When it is applicable, what is the appropriate K_{pt}? What isotherms apply when the Langmuir form does not? In this section we will address the first question and set the stage for our subsequent discussion of the remaining two.

By definition the Langmuir isotherm applies to equilibrium states. When using it, it is necessary first to establish that x_{eq} is stationary in time and does not vary with sample preparation; i.e., there is no hysteresis. Beyond the equilibrium and small spot conditions, other requirements are imposed by the assumptions underlying the derivation of the Langmuir isotherm (1). In the language of DNA chips the following additional conditions must be satisfied.

(1) A spot should carry only one type of probe. In other words, the probes within a given spot should be perfectly monodispersed in size and sequence.
(2) Each probe species can hybridize only with a single, unique target. This is actually the case for single-component hybridization solutions and for perfectly selective probes.

(3) A target cannot hybridize with complementary strands in the solution; i.e., the sample comprises non-complementary ssDNA. Similarly, self-hybridization and the formation of hairpins and loops are also prohibited.
(4) Each target hybridizes with a single probe. In other words the length and sequence of the target and the separation between the probes rule out the possibility of a single target hybridizing with two separate probes.
(5) There is no interaction between the probes irrespective of their hybridization state. Stated differently, the in-plane separation between the probes must be large compared to the range of their interactions. In particular, this rules out situations where the density of the probes at the surface allows for two probes to hybridize with each other or leads to steric hindrance between the hybridized probes. Similarly the separation should exceed the range of excluded volume and electrostatic interactions.

In many realistic situations these requirements are not fulfilled: *in situ* synthesis leads to probe polydispersity, while samples of dsDNA introduce a competitive hybridization reaction in the bulk. In the case of RNA samples self-hybridization also leads to bulk competitive hybridization. In samples of biological origin, different targets can hybridize with the same probe. Such surface competition is a critical factor when somatic point mutations are studied. This is due to the presence of an excess of wild-type DNA. Finally, high surface densities of probes introduce interactions between the probes. These can assume a number of forms. When the surface area per probes is comparable to the cross section of the dsDNA, steric hindrance of the hybridization is important. In this regime neighbouring self-complementary probes can also hybridize among themselves. At lower surface densities the probes, hybridized or not, undergo both electrostatic and excluded volume interactions.

When the Langmuir isotherm is applicable, it is necessary to specify the equilibrium constant K_{pt}. This brings us to the second question: what is K_{pt}? It is often assumed that K_{pt} is well approximated by

$$K_{pt}^{0} = \exp\left(-\frac{\Delta G_{pt}^{0}}{RT}\right) \tag{3}$$

where the free energy ΔG_{pt}^{0} is obtained from the nearest neighbour (NN) method [43–46], T is the temperature and $R = 8.314\ \mathrm{J\,mol^{-1}\,K^{-1}}$ is the gas constant. Within the NN method, ΔG_{pt}^{0} is obtained by summing the contributions of nearest neighbour base pairs, allowing also for those of dangling ends and of an initiation term. In particular, the enthalpy is $\Delta H_{pt}^{0} = \Delta H_{\mathrm{init}} + \sum_{i=1}^{n-1} \Delta H_i$ where each ΔH_i denotes the contribution of the $(i, i+1)$ base pair while ΔH_{init} reflects the initiation. The different possible ΔH_i are determined experimentally. Similar expressions yield the entropy ΔS_{pt}^{0}, thus allowing one to obtain ΔG_{pt}^{0}. The use of this approximation introduces further assumptions. First, by construction the NN method does not allow for the long ranged, excluded volume interactions between the bases. It thus assumes that the ssDNA adopts the configuration of an ideal, Gaussian coil. Second, the K_{pt}^{0} thus obtained is identical to the bulk equilibrium constant. It does not reflect the effect of the impenetrable wall which reduces the number of accessible configurations to a chain at the surface. Third, the NN method allows for the hybridized base pairs and, at most, two dangling ends. It thus predicts an identical K_{pt}^{0} for all probe–target pairs such that $N_t \geqslant n+2$. This result is reasonable only for free Gaussian strands in the bulk. Finally, since the NN method is based on a two-state model for the hybridization, it is only applicable to passivated surfaces when neither the ssDNA nor the dsDNA can adsorb and to short chains. This last point, and the neglect of the excluded volume effect, limit the reliability range of the NN method to oligonucleotide probes of length

$n \lesssim 20$. The points listed above suggest that the real equilibrium constant, K_{pt}, may well differ from K^0_{pt} obtained from the NN method.

The modifications resulting from the various effects listed above will be discussed in detail in sections 4–8. In the remainder of this section we comment on the ensuing differences in the formulation of the problem. To facilitate the discussion of K_{pt} versus K^0_{pt} and the various forms of the hybridization isotherms it is helpful to recall the derivation of the Langmuir isotherm. It is obtained from the equilibrium condition of the hybridization reaction, $p + t \rightleftharpoons pt$. In particular $\mu_{pt} = \mu_p + \mu_t$ where μ_i is the chemical potential of species i. The assumption that the NN method describes the hybridization reaction specifies the standard state, or μ^0_i, so $\mu^0_{pt} - \mu^0_p - \mu^0_t = \Delta G^0_{pt}$. As discussed earlier, within this approach the chains are assumed to be ideal Gaussian coils experiencing neither excluded volume interactions nor the effects of the impenetrable wall. The target solution is dilute and the ionic strength of the solution is high. Accordingly, electrostatic interactions between the targets are screened and μ_t assumes the weak solution form. To obtain (1) it is necessary to invoke the small spot limit, assuming that the number of targets is much bigger than the number of corresponding probes. As a result the initial molar concentration of the targets, c_t, is only weakly diminished by the hybridization reaction and the target concentration is well approximated by c_t. Altogether $\mu_t = \mu^0_t + RT \ln c_t$. To obtain μ_{pt} and μ_p it is necessary to specify the surface free energy per probe site, $\gamma_{\rm site}$, as a function of x, the fraction of hybridized probes. The pt and p chains form a two-dimensional solution associated with a mixing entropy of $-R[x \ln x + (1-x)\ln(1-x)]$ per probe site. Within the NN method and when there are no interactions between the probes irrespective of their hybridization state, $\gamma_{\rm site}$ is

$$\gamma^0_{\rm site}(x) = x\mu^0_{pt} + (1-x)\mu^0_p + RT[x \ln x + (1-x)\ln(1-x)] \tag{4}$$

up to an additive constant. To obtain the Langmuir isotherm it is convenient to express the equilibrium condition $\mu_{pt} = \mu_p + \mu_t$ in terms of the exchange chemical potential of the hybridized probe, $\mu^{\rm ex}_{pt} = \mu_{pt} - \mu_p = \partial\gamma^0_{\rm site}/\partial x$, thus leading to $\mu^{\rm ex}_{pt} = \mu_t$ and to equation (1). For simplicity, our subsequent discussion focuses on the small spot limit noting that it is straightforward to correct for deviations from this regime [38].

How do the various effects considered above manifest themselves? When a single hybridization reaction is involved, two modifications come into play. The first concerns the μ^0_i. For the targets μ^0_t may be replaced by $\mu^0_t + \overline{\mu}_t$ where $\overline{\mu}_t$ allows for excluded volume interactions. Similarly μ^0_p and μ^0_{pt} are supplemented by terms, $\overline{\mu}_p$ and $\overline{\mu}_{pt}$, allowing for the effects of the impenetrable wall on chains that do not interact with each other. These two terms assume different forms for ideal chains behaving as random walks (RW) and for chains experiencing excluded volume interactions, which exhibit the statistics of self-avoiding random walks (SAW). A second modification is required for sufficiently small Σ_0 when interactions between probe sites give rise to an extra term, $G_{\rm int}(x)$, in $\gamma_{\rm site}$. This last term also reflects the corresponding modifications of the wall effects. Altogether,

$$\gamma_{\rm site}(x) = \gamma^0_{\rm site}(x) + x\overline{\mu}_{pt} + (1-x)\overline{\mu}_p + G_{\rm int}(x) \tag{5}$$

and the hybridization isotherm assumes the form

$$\frac{x_{\rm eq}}{1-x_{\rm eq}} = c_t K_{pt} \exp\left(-\frac{1}{RT}\frac{\partial G_{\rm int}}{\partial x}\right) = c_t K_{pt} f(x_{\rm eq}) \tag{6}$$

where

$$K_{pt} = K^0_{pt}\overline{K}_{pt} = K^0_{pt} \exp\left(-\frac{\Delta\overline{G}_{pt}}{RT}\right) \tag{7}$$

and $\overline{\mu}_{pt} - \overline{\mu}_p - \overline{\mu}_t = \Delta\overline{G}_{pt}$. Importantly K^0_{pt} depends only on the sequence and length of the probe while $\overline{K}_{pt}$ is essentially sequence independent but varies with n, N_t and the spacer length. The $f(x_{\rm eq})$ factor, that differs from unity only when the interactions between probe sites are non-negligible, is also dependent on Σ_0. When two or more hybridization reactions occur it is necessary to allow for additional chemical species and equilibrium conditions. As we shall see, these lead to deviations from the form (6).

3. On probe design and data analysis: $T_{\rm m}$ versus c_{50}

The Langmuir isotherm defines two characteristics of the surface hybridization reaction. One is the melting temperature $T_{\rm m}$ for which half of the probes are hybridized or $x_{\rm eq} = 1/2$, as defined via the condition $\ln\left(c_t K_{pt}\right) = 0$. The second is a characteristic concentration, c_{50}, specified by $x_{\rm eq} = 1/2$ or

$$c_{50} = 1/K_{pt}. \tag{8}$$

$T_{\rm m}$ varies with c_t while c_{50} is a function of T. Lowering the hybridization temperature with respect to $T_{\rm m}$ increases $x_{\rm eq}$ and thus the signal. On the other hand a lower T also stabilizes probes hybridized to mismatched targets with a consequent lower stringency. The significance of c_{50} is apparent when the Langmuir isotherm is expressed as

$$x_{\rm eq} = \frac{c_t/c_{50}}{1 + c_t/c_{50}}. \tag{9}$$

In particular (i) the linear adsorption regime, $x_{\rm eq} \sim c_t$, is obtained when $c_t \ll c_{50}$, (ii) the saturation behaviour, $x \to 1$, occurs when $c_t \gg c_{50}$ and finally (iii) $1/c_{50}$ is a measure of the sensitivity of the assay [38]. This is clearly evident in the $c_t \ll c_{50}$ range when $x_{\rm eq} \approx c_t/c_{50}$. The two characteristics, $T_{\rm m}$ and c_{50}, while related, are different and complementary. The relationship between the two is best examined for their NN version.

The melting temperature as obtained via the NN method is

$$T^0_{\rm m}(c_t) = \frac{\Delta H^0_{pt}}{\Delta S^0_{pt} + R\ln c_t}. \tag{10}$$

This definition differs slightly from the one obtained for the bulk melting temperature because the probes are now immobilized at the surface. In particular, c_t should be replaced by $c_t/4$ when calculating the bulk melting temperature. The bulk version of $T^0_{\rm m}(c_t)$ is often used in the design of probe sequences via the requirement that all probes have similar $T^0_{\rm m}$. The corresponding c_{50} is

$$c^0_{50} = 1/K^0_{pt} = \exp\left(\Delta G^0_{pt}/RT\right). \tag{11}$$

It is first important to note that two probe–target pairs with identical $T^0_{\rm m}$ do not necessarily have equal c^0_{50}. This is clear upon expressing ΔG^0_{pt} as $(T^0_{\rm m} - T)\Delta S^0_{pt}$ where we have utilized, for simplicity, $T^0_{\rm m}$ as obtained for $c_t = 1$ M. Clearly, ΔG^0_{pt} of different probe–target pairs having equal $T^0_{\rm m}$ will be identical only at $T = T^0_{\rm m}$. For $T \neq T^0_{\rm m}$ the two ΔG^0_{pt} will differ whenever the two ΔS^0_{pt} are unequal, as is generally the case.

As noted earlier, the current practice is to choose probes with similar $T^0_{\rm m}$ without checking for the proximity of the corresponding c^0_{50} values [41]. The c^0_{50} s are however important because they determine the intensities of the spots. For the case of two probes, i and j, hybridizing with an identical target the ratio of the two $x_{\rm eq}$ in the linear regime is

$$\frac{x_{\rm eq}(i)}{x_{\rm eq}(j)} = \frac{I_i}{I_j}\frac{I_{\rm max}(j)}{I_{\rm max}(i)} = \frac{c^0_{50}(j)}{c^0_{50}(i)}. \tag{12}$$

Table 1. Comparison of the c_{50}^0 of probes with similar T_m^0 ($T = 50\,^\circ$C, 1 M NaCl).

Probe position	ΔH_{pt}^0 (kcal mol^{-1})	ΔS_{pt}^0 (cal mol^{-1} K^{-1})	T_m ($^\circ$C)	c_{50}^0 (10^{-18} M)
401	−229.0	−630.7	59.5	9.2
411	−230.9	−631.2	62.0	0.61
521	−228.7	−624.9	61.9	0.79

In other words, in the ideal case of two spots incorporating identical number of probes, $I_i/I_j = c_{50}^0(j)/c_{50}^0(i)$. This observation has important consequences for probe design and for the normalization of the data. To illustrate this point we compare the c_{50}^0 of three probes selected on the basis of the proximity of the melting temperatures [41]. The example concerns the search for $n = 30$ probes for the 600 bp *Homo sapiens* alcohol dehydrogenase beta2 subunit gene. The selection process first minimizes sequence homology among the probes. Table 1 lists the thermodynamic parameters of the three selected probes chosen, additionally, to have $T_m = 60\,^\circ$C within $\pm 2\,^\circ$C and following the elimination of probes with significant self-complementarity. Importantly, the three candidates are equivalent within this selection scheme. The probes are identified by their position as specified by the distance, in number of bases, of the 5′ base of the probe from the 3′ end of the target. The table specifies ΔH_{pt}^0, ΔS_{pt}^0, T_m as obtained for $c_t = 1$ pM and the c_{50}^0 calculated for a hybridization temperature $T = 50\,^\circ$C. As we see from the table the ratio of the c_{50}^0 of the 411 and 521 probes is close to unity while the ratio of c_{50}^0 of the 401 and 521 probes is of order 10. This implies that the equilibrium signal from the 401 spot, all other factors being equal, will be roughly ten times weaker. Importantly, it is straightforward to supplement the current probe selection method to incorporate the requirement of similar c_{50}^0 values. This will eliminate a source of variation in the intensity of the spots and facilitate the subsequent data treatment.

4. The effect of the impenetrable wall on K_{pt}: glass slides versus gel pads

In its original incarnation the Langmuir isotherm described the adsorption of a gas onto a solid substrate. In this situation the equilibrium constant had no bulk counterpart involving free reactants in solution. In contrast, for DNA chips the hybridization of free single-stranded NA specifies a natural reference state. In view of the extensive data compiled on the solution reaction it is useful to understand the relationship between the equilibrium constants at the surface and in the bulk. The two situations, bulk and surface, are qualitatively different when the probes are terminally anchored onto a glass slide or a silicon wafer. In these cases, the surface is an impenetrable wall affecting the number of configurations available to the chain. The difference is much smaller when the probes are bound to a gel pad [47]. In this last case, the number of accessible configurations is hardly modified though the solvent quality may be affected. In the following we consider the impenetrable wall scenario with a view to comparing the equilibrium constants in the bulk and at the surface. Focusing on the large Σ_0 limit, two sources of differences between the equilibrium constants come to mind. The presence of an impenetrable wall and the possibility of NA adsorption at the surface. Since suitable surface treatment can repress adsorption we limit the discussion to the intrinsic role of the impenetrable surface.

The number of configurations accessible to a polymer is reduced when it is terminally anchored to an impenetrable surface (figure 2). In turn, this affects the hybridization constant at the surface. The effect of the wall varies with the rigidity of the chain. In the range of n and N_t encountered in experiments involving oligonucleotide chips, ssDNA behaves as a

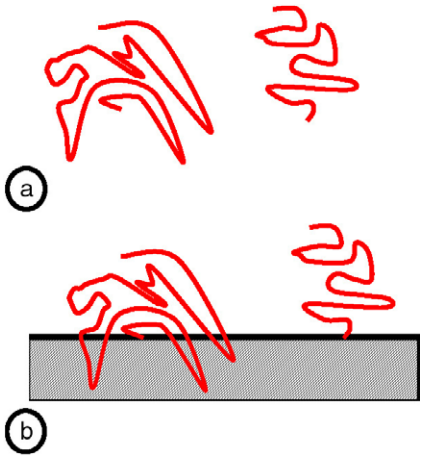

Figure 2. Tethering chains onto an impenetrable surface reduces the number of accessible chain configurations; (a) schematically depicts two possible bulk configurations of which only one survives when the chain is terminally anchored as shown in (b).

semiflexible chain while dsDNA may be viewed as a rigid rod. To understand the effect of the impenetrable wall on the hybridization behaviour it is helpful to recall exact results [48, 49] concerning the asymptotic form of the number of configurations available to a single chain. The number of configurations of a free flexible chain comprising N monomers is

$$Z_{\text{free}} = z^N N^{\gamma-1} \tag{13}$$

while for a chain terminally anchored to a planar impenetrable surface

$$Z_{\text{mushroom}} = z^N N^{\gamma_s-1} \tag{14}$$

where z is a system dependent constant. This situation corresponds to the case of large Σ_0 so as to ensure that the chains do not interact. For random walks (RW) on a lattice, z is identical to the coordination number of the lattice. For self-avoiding random walks (SAW) z is replaced by $\tilde{z} < z$. The exponents γ and γ_s are universal and depend only on the dimensionality. In three-dimensional systems $\gamma = 1$ for RW and $\gamma \simeq 1.167$ for SAW. The corresponding values for γ_s are $\gamma_s = 1/2$ (RW) and $\gamma_s \simeq 0.695$ (SAW). In both cases, $Z_{\text{mushroom}} < Z_{\text{free}}$. Anchoring to an impenetrable wall also reduces the number of configurations accessible to a rigid rod. In this case, the effect depends on the nature of the anchoring group. In the following we consider the case of a rod anchored to a surface via a short flexible spacer. In other words, the rod can rotate freely around the grafting site. Accordingly, the free end of the rod can explore the envelope of a hemisphere while the tip of a free rod explores the surface of a sphere. The corresponding numbers of configurations are proportional respectively to 2π and 4π. In contrast to the case for a flexible chain, the effect is independent of the length of the rod and we will thus neglect this constant term.

To simplify the discussion we consider the effect of the impenetrable wall on the hybridization equilibrium when a ssDNA behaves as an ideal Gaussian chain exhibiting RW statistics. Initially we ignore the effect of the persistence length. It is convenient to examine the ratio of hybridization equilibrium constants at the surface and in the bulk:

$$\frac{K_{pt}(\text{surface})}{K_{pt}(\text{bulk})} = \frac{K_{pt}}{K_{pt}^0} = \overline{K}_{pt}. \tag{15}$$

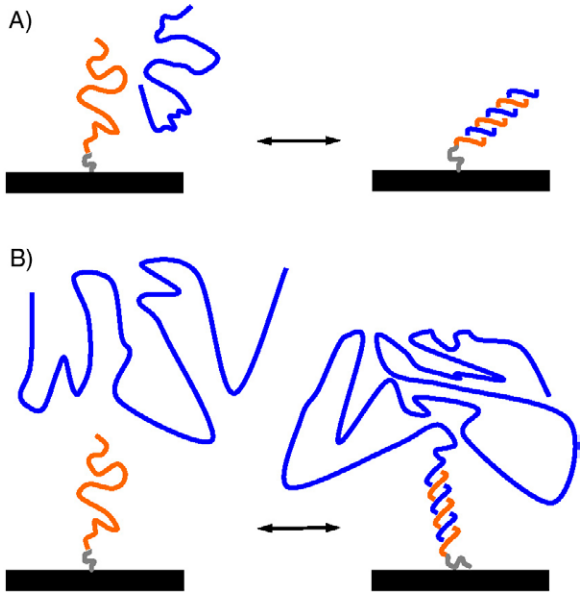

Figure 3. (A) The hybridization constant at the surface is larger than the bulk one for $N_t = n$ because of the reduced entropy of the probes. (B) The opposite trend is expected for $N_t \gg n$ because of the entropy loss of the ssDNA tail of the hybridized probes.

We first consider the case of $N_t = n$ (figure 3(A)). Since ssDNA is assumed to behave as an ideal chain $\overline{\mu}_t = 0$. In view of our earlier discussion of rigid rods we make the approximation $\overline{\mu}_{pt} = 0$. The effect of the impenetrable surface manifests itself via $\overline{\mu}_p = RT \ln n^{1/2}$, thus leading to

$$\overline{K}_{pt} = n^{1/2} \qquad \text{for } N_t = n. \tag{16}$$

Since the ssDNA is semiflexible, $n^{1/2}$ should be replaced by $(na/l_p)^{1/2}$ where l_p is the persistence length and a the monomer or base size. In the $N_t = n$ case the impenetrable surface favours the hybridization because the entropy of one of the reactants, the probes, is reduced. The opposite effect occurs for long targets, $N_t \gg n$ (figure 3(B)). As before, $\overline{\mu}_t = 0$ and $\overline{\mu}_p = RT \ln n^{1/2}$. However, $\overline{\mu}_{pt}$ must now account for the effect of the impenetrable wall on the non-hybridized tail of pt. The tail is anchored to the surface via a dsDNA segment of length $\sim n$ thus leading to $\overline{\mu}_{pt} = RT \ln N_t^{1/2}/n$ and

$$\overline{K}_{pt} = n\left(\frac{n}{N_t}\right)^{1/2} \qquad \text{for } N_t \gg n. \tag{17}$$

Here the effect of the persistence length is cancelled out and N_t approximates $N_t - n$, the number of unhybridized bases in the target [40]. The reduced entropy of the products, pt, can overwhelm the lower entropy of the reactant p, thus leading to a smaller $\overline{K}_{pt}$. Note that the modifications in $\overline{K}_{pt}$ indicate that the rate constants at the surface differ from the bulk values [40].

While our analysis captures an essential ingredient of the system, it is important to underline its limitations. First, our argument utilizes asymptotic expressions for $Z(N)$ that apply when N is large. Their applicability to short oligonucleotides is not clear. Second, $Z(N)$ actually depends on the number of Kuhn lengths rather than the number of bases, monomers. In turn, the precise values of the persistence length of ssDNA remain to be established [50–52].

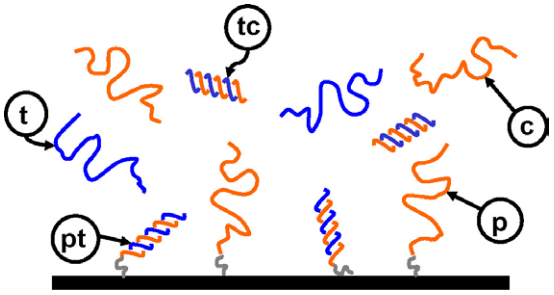

Figure 4. A schematic picture of bulk competition due to the hybridization of the targets with free complementary ssDNA in the solution.

Third, the onset of self-avoidance in ssDNA is also in need of study. It is thus possible that long targets behave as SAW while the short probes exhibit Gaussian behaviour. Finally, it is important to stress that the analysis, as presented above, applies only to the case of non-adsorbing surfaces.

5. Competitive bulk hybridization: double-stranded versus single-stranded targets

The Langmuir isotherm (1) is realized when a single-stranded target, t, hybridizes with probes of a single type, p, in the weak spot limit. As noted earlier, a single hybridization reaction is involved. This behaviour is modified when a number of different hybridization reactions take place. In this section we consider the effect of competitive hybridization reactions occurring in the bulk solution rather than at the surface. Two extreme types of bulk hybridization reaction are possible: intermolecular hybridization of the target with its complement (figure 4) and intramolecular, self-hybridization resulting in the formation of hairpins or loops. In both cases we can no longer assume that the concentration of free targets $[t]$ is identical to its initial concentration, c_t. Instead $c_t > [t]$ because the concentration of target available for hybridization at the surface is lowered by the competitive hybridization reactions. Accordingly the hybridization isotherm (1) becomes

$$\frac{x_{\mathrm{eq}}}{1 - x_{\mathrm{eq}}} = [t]K_{pt}. \tag{18}$$

We first discuss the intermolecular case and then comment on the effect of self-hybridization. In both cases we limit the analysis to the simplest case of non-interacting probes and the absence of competitive surface hybridization.

In experiments probing genomic DNA the sample may comprise dsDNA or a mixture of dsDNA and ssDNA. This last case is realized, for example, when asymmetric PCR is used to amplify the DNA. In these situations, each t strand can undergo two reactions: $p + t \rightleftharpoons pt$ at the surface and bulk intermolecular hybridization with the complementary sequence c following $t + c \rightleftharpoons tc$. The mass action law for the bulk reaction is $[tc]/[t][c] = K_{\mathrm{bulk}}$ where $[i]$ is the equilibrium concentration of i and K_{bulk} is the equilibrium constant of the reaction for the temperature and ionic strength considered. Importantly, $K_{\mathrm{bulk}}(N_t)$ describes the hybridization equilibrium between strands comprising N_t bases and in biology experiments $N_t \gg n$. This mass action law is supplemented by the conservation relations $[t] + [tc] = c_t$ and $[c] + [tc] = c_c$ where c_i denotes the total concentration of i. In the general case $[t]$ is specified by $K_{\mathrm{bulk}}[t]^2 + \{K_{\mathrm{bulk}}(c_c - c_t) + 1\}[t] - c_t = 0$ [28]. For simplicity we now consider the typical case of a dsDNA sample when $c_t = c_c$. In the small spot limit, the mass action law

for the bulk hybridization is

$$\frac{\alpha}{(1-\alpha)^2} = \frac{2c_t}{c_{1/2}} \tag{19}$$

where $\alpha = [tc]/c_t$ and

$$c_{1/2} = 2/K_{\text{bulk}} \tag{20}$$

is the t concentration leading to 50% bulk hybridization at a particular temperature, ionic strength etc. When $c_t \ll c_{1/2}$ the effect of the bulk hybridization is negligible, $[t] \approx c_t$ and the Langmuir form of the hybridization isotherm (1) is recovered. In the opposite case, $c_t \gg c_{1/2}$, the bulk hybridization leads to strong deviation from the Langmuir behaviour. As we shall discuss, this deviation is important in experiments involving long targets and a hybridization temperature significantly lower than the bulk melting temperature of the ds tc. In this situation $[t] \approx \sqrt{c_{1/2}c_t/2}$, thus leading to

$$\frac{x_{\text{eq}}}{1-x_{\text{eq}}} = \sqrt{\frac{c_t}{c_{50}^{bc}}} \tag{21}$$

where c_{50}^{bc} is the t concentration corresponding to 50% hybridization at the surface. The competitive hybridization results in $[t] < c_t$ and as a consequence $c_{50}^{bc} > c_{50}$, thus indicating lower sensitivity. When bulk hybridization is important,

$$c_{50}^{bc} = K_{\text{bulk}}c_{50}^2 = \frac{2c_{50}^2}{c_{1/2}}. \tag{22}$$

The dependence of x_{eq} on c_t in this case assumes the form

$$x_{\text{eq}} = \frac{\sqrt{c_t/c_{50}^{bc}}}{1+\sqrt{c_t/c_{50}^{bc}}}. \tag{23}$$

When $c_{1/2} \ll c_t \ll c_{50}^{bc}$, or $c_{50}^{bc}/c_{1/2} = K_{\text{bulk}}^2/2K_{pt}^2 \gg 1$, the hybridization isotherm reduces to

$$x_{\text{eq}} = \sqrt{c_t/c_{50}^{bc}}. \tag{24}$$

When (1) is applicable, the spot intensity I for $c_t \ll c_{50}$ is proportional to x_{eq}, thus leading to $I \sim c_t$. In marked contrast, (24) leads to $I \sim \sqrt{c_t}$. The importance of this effect varies with the span of the applicability range $c_{1/2} \ll c_t \ll c_{50}^{bc}$ which depends, in turn, on n and N_t. A simple estimate of the span of the $I \sim \sqrt{c_t}$ regime is possible when the targets and the probes behave as Gaussian chains. For $N_t = n$ the hybridization constant at the surface $K_{pt} = (na/l_{\text{p}})^{1/2}K_{pt}^0$ is larger than the bulk hybridization constant $K_{\text{bulk}} = K_{pt}^0$. Accordingly $c_{50}^{bc}/c_{1/2} \approx l_{\text{p}}/an < 1$ and the $I \sim \sqrt{c_t}$ regime is not observable. The applicability range when $N_t \gg n$ is wide because $c_{50}^{bc}/c_{1/2} = 2(N_t/n)^{1/2}K_{\text{bulk}}(N_t)/K_{pt}^0(n) \gg 1$ since both $K_{\text{bulk}}(N_t)/K_{pt}^0(n) \gg 1$ and $(N_t/n)^{1/2} \gg 1$. When $N_t \geqslant 100$ as is often the case for bioanalytical experiments, it is difficult to estimate $K_{\text{bulk}}(N_t)$ because the two-state assumption, underlying the NN method, is no longer valid. Numerical calculations for the $x_{\text{eq}} \sim \sqrt{c_t}$ regime are however possible (figure 5) for Gaussian chains with $N_t \leqslant 30$ and $n \approx 20$, a range that is easily accessible to physical chemistry-type experiments. With the reservations noted above the $I \sim \sqrt{c_t}$ behaviour is significant in experiments involving quantitative genotyping of pooled samples [53] as used to determine the frequency distribution of single-nucleotide polymorphism in a selected population.

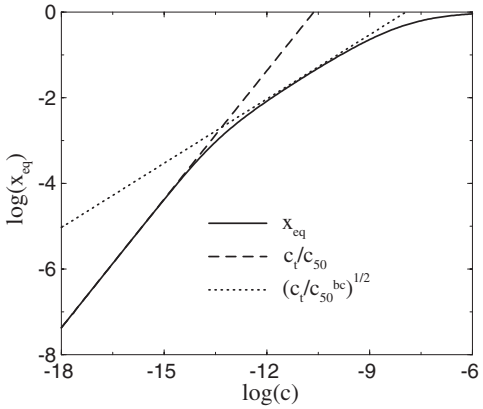

Figure 5. The hybridization isotherm when the bulk hybridization reaction involves targets longer than the probes and the $I \sim \sqrt{c_t}$ regime is important. In this calculation $n = 20$, $N_t = 25$ and $T = 60\,^{\circ}\mathrm{C}$. The probe sequence is 5′-AGATTGCAAATACTGCCCGC-3′ and the target sequence is 5′-CGTTTGCGGGCAGTATTTGCAATCT-3′, thus leading to $\Delta H^0_{pt} = -161.50$ kcal mol^{-1}, $\Delta S^0_{pt} = -436.37$ cal mol^{-1} K^{-1}, $\Delta H^0_{tc} = -199.90$ kcal mol^{-1} and $\Delta S^0_{\mathrm{tc}} = -539.38$ cal mol^{-1} K^{-1} as determined from the NN method [43–46]. For $c_t < c_{1/2} = 48$ fM, the hybridization isotherm (full line) follows the linear regime $x \approx c_t/c^0_{50}$ (dashed line) with $c^0_{50} = 23$ pM. For $c_{1/2} < c_t < c^{bc}_{50} = 11$ nM, it follows $x \approx \sqrt{c_t/c^{bc}_{50}}$ (dotted line), while for $c_t > c^{bc}_{50}$ an onset of saturation behaviour occurs.

Intramolecular self-hybridization also results in $[t] < c_t$. In this case the bulk hybridization is unimolecular, $t \rightleftharpoons h$, where h denotes the self-hybridized t whose hybridization site with p is blocked because of the formation of the hairpin. The mass action law in this case is $[h]/[t] = K_h$ and the conservation law is $[h] + [t] = c_t$, thus leading to

$$[t] = \frac{c_t}{1 + K_h} \tag{25}$$

where K_h is the equilibrium constant for the formation of hairpins. As a result, the hybridization isotherm retains the Langmuir form (1) but K_{pt} is modified and the isotherm exhibits a lower effective hybridization constant:

$$\frac{x_{\mathrm{eq}}}{1 - x_{\mathrm{eq}}} = c_t \frac{K_{pt}}{1 + K_h}. \tag{26}$$

This leads, as expected, to a lower sensitivity as indicated by the higher value of the corresponding $c^h_{50} = (1 + K_{\mathrm{h}})c_{50}$. This effect is significant for RNA targets which are prone to self-hybridization but may also affect the hybridization isotherms of ssDNA.

6. Competitive surface hybridization: multicomponent solutions

In biology experiments the DNA chip is placed into contact with a solution of many different NA sequences, cDNA or cRNA depending on the experimental protocol. Different targets may hybridize with the same probe species, that is, at the same spot. This competitive surface hybridization can be beneficial or detrimental. The role depends on the experimental design and, in particular, on the labelling scheme. To begin with, we discuss the general features of the competitive surface hybridization for the case of two surface reactions $p + t \rightleftharpoons pt$ and $p + \overline{t} \rightleftharpoons p\overline{t}$ (figure 6). The generalization to a case involving a larger number of reactions

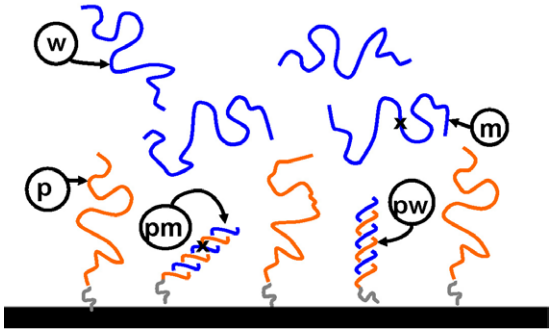

Figure 6. Surface competitive hybridization as it occurs when two different targets, denoted by w and m, can hybridize with the same probe.

is straightforward. For simplicity we limit the discussion to systems with no interactions or competitive bulk hybridization, i.e., large Σ_0 and sample of non-complementary ssDNA targets. We will later consider the consequences for two special cases: two-colour experiments and the detection of somatic point mutations as markers of cancer.

Three hybridization isotherms specify the equilibrium behaviour of the system. They relate the fractions of pt and $p\bar{t}$, denoted respectively by x and y, to the concentrations of the two competing targets, c_t and $c_{\bar{t}}$. In the absence of interactions and bulk competition, $x_{\rm eq}$ and $y_{\rm eq}$ are specified by [38]

$$\frac{x_{\rm eq}}{1-(x_{\rm eq}+y_{\rm eq})} = c_t K_{pt}, \tag{27}$$

$$\frac{y_{\rm eq}}{1-(x_{\rm eq}+y_{\rm eq})} = c_{\bar{t}} K_{p\bar{t}}. \tag{28}$$

Accordingly, the total hybridization isotherm for the spot is

$$\frac{x_{\rm eq}+y_{\rm eq}}{1-(x_{\rm eq}+y_{\rm eq})} = c_t K_{pt} + c_{\bar{t}} K_{p\bar{t}} \tag{29}$$

as obtained by summing (27) and (28). In physical chemistry experiments it is possible to selectively label t and $\bar{t}$ as well as control c_t and $c_{\bar{t}}$. Accordingly, such experiments can validate all three isotherms. In biology experiments, in contrast, the concentrations are unknown quantities to be determined and selective labelling is impossible. As a result, only isotherm (29) is observable in such experiments.

Competitive surface hybridization is utilized to advantage in two-colour experiments. In these, two cDNA samples are labelled with different dyes. The two typical dyes are cyanine 3 and 5 giving rise, respectively, to green and red fluorescence. The two samples are mixed in equal proportions and the resulting mixture is hybridized with the oligonucleotide chip. Each spot thus undergoes two competitive surface hybridization reactions $p + t\,({\rm g}) \rightleftharpoons pt\,({\rm g})$ and $p + t\,({\rm r}) \rightleftharpoons pt\,({\rm r})$ where $t\,({\rm g})$ and $t\,({\rm r})$ denote targets labelled respectively with green and red dyes. Note that our formulation of the problem assumes, for simplicity, perfectly selective probes, i.e., probes that only hybridize with perfectly complementary targets. The ratio of isotherms (27) and (28) yields

$$\frac{x_{\rm eq}}{y_{\rm eq}} = \frac{c_t({\rm g})K_{pt}({\rm g})}{c_t({\rm r})K_{pt}({\rm r})} \tag{30}$$

where $x_{\rm eq} = I({\rm g})/I_{\rm max}({\rm g})$ and $y_{\rm eq} = I({\rm r})/I_{\rm max}({\rm r})$. Here $I(i)$ is the intensity of the colour i and $I_{\rm max}(i)$ is the corresponding maximal attainable intensity at saturation. Importantly,

$I_{\max}(i)$ specifies the saturation upon hybridization with a single-component solution of $t(i)$, in the absence of competition. Both $I_{\max}(i)$ are proportional to the number of probes within the spot. However, the two are typically different because the corresponding dyes differ in their extinction coefficients, quantum yields and reactivities. The hybridization of labelled targets may well differ from that of unlabelled ones. Since the two dyes differ in molecular structure and reactivity it is necessary to introduce distinct equilibrium constants, $K_{pt}(\mathrm{g})$ and $K_{pt}(\mathrm{r})$. Altogether

$$\frac{I(\mathrm{g})}{I(\mathrm{r})} = \frac{c_t(\mathrm{g})I_{\max}(\mathrm{g})K_{pt}(\mathrm{g})}{c_t(\mathrm{r})I_{\max}(\mathrm{r})K_{pt}(\mathrm{r})} \tag{31}$$

and a simple equality $I(\mathrm{g})/I(\mathrm{r}) = c_t(\mathrm{g})/c_t(\mathrm{r})$ is only attained for ideal systems with $I_{\max}(\mathrm{g}) = I_{\max}(\mathrm{r})$ and $K_{pt}(\mathrm{g}) = K_{pt}(\mathrm{r})$. It is important to note that $I_{\max}(\mathrm{g})/I_{\max}(\mathrm{r})$ for a single spot is independent of the number of probes in the spot and may thus be determined from the known properties of the dyes. Accordingly, two-colour experiments yield, ideally, the relative levels of gene expression in a sample as compared to the chosen reference. Comparison of expression levels of different genes is however hampered by the necessity to specify the ratio of the number of probes in the corresponding spots.

In contrast to the case for two-colour experiments, competitive surface hybridization plays a negative role in experiments aiming to utilize somatic point mutations as markers for cancer [39]. In this situation the biological sample contains a mixture of wild-type DNA (w), associated with normal cells, and DNA with point mutations from the cancerous ones. Importantly, all species are labelled with the same dye. Furthermore, the wild-type DNA is present in large excess [53], especially when screening for cancer using biological fluids such as blood or stool [54]. To illustrate the negative role of the competitive surface hybridization we consider the hybridization at a spot corresponding to a point mutation m. The hybridization at this spot is due to two competitive reactions $p+m \rightleftharpoons pm$ and $p+w \rightleftharpoons pw$. The contribution of the second reaction is significant because the large excess of w favours the formation of pw even though $K_{pw} < K_{pm}$. Since selective labelling is impossible, the observed isotherm is (29). The contribution of pw to the total signal of the spot, as obtained from the ratio of (28) and (29), is

$$P = \frac{y_{\mathrm{eq}}}{x_{\mathrm{eq}} + y_{\mathrm{eq}}} = \frac{K_{pw}c_w}{K_{pm}c_m + K_{pw}c_w}. \tag{32}$$

Importantly the fraction of mishybridized probes $P > 1/2$ whenever $c_w/c_m > K_{pm}/K_{pw}$. A signal is clearly expected even when $c_m = 0$, thus demonstrating that a bright mutation spot is not necessarily an indication of cancer (figure 7). To eliminate the risk of false positives it is necessary to determine both x_{eq} and y_{eq}. This may be achieved, for example, by measuring the equilibrium hybridization signal at two different temperatures [39]. It is also useful to note that the melting temperature of a probe layer undergoing competitive surface hybridization is not given by (10). Rather it is a non-linear function of c_m and c_w [39].

7. Polydispersity of probes and targets

Polydispersity of both the probes and the targets is often encountered in experiments involving DNA chips. The polydispersity of probes in a given spot is an inherent result of the reaction yields utilized for *in situ* synthesis. Target polydispersity is the outcome of target fragmentation. In both cases, the observed signal reflects the overall hybridization and it is currently impossible to separate the contributions of the different components involved. It is useful to note that each of the two polydispersities affects the hybridization isotherms in a distinctive fashion. Target

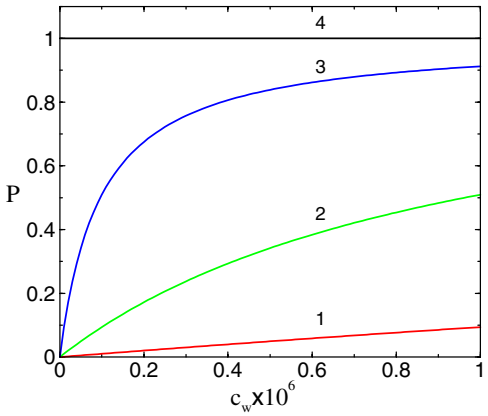

Figure 7. Because of competitive surface hybridization the hybridization at a spot is due to both the perfect complement of the probe and the mismatched one. The fraction of mishybridized probes, P, is plotted for the case of a spot carrying probes for the mutation Ala12 on the gene *K-ras* with sequence 5′-AGCTGCTGGCGTA-5′ contacted with a solution containing both mutated (5′-TACGCCAGCAGCT-3′) and wild-type targets (5′-TACGCCACCAGCT-3′) with concentrations c_m and c_w [54, 39]. The thermodynamic parameters for the perfect match $\Delta H^0_{pm} = -99.40$ kcal mol^{-1} and $\Delta S^0_{pm} = -264.29$ cal mol^{-1} K^{-1} and the mismatch $\Delta H^0_{pw} = -78.20$ kcal mol^{-1} and $\Delta S^0_{pw} = -214.12$ cal mol^{-1} K^{-1} are determined from the NN method [43–46]. The four curves correspond to $c_m = 1$ μM (1), 100 pM (2), 10 pM (3) and 0 M (4). The hybridization temperature is 47 °C.

polydispersity gives rise to competitive surface hybridization as discussed before. The effect of probe polydispersity is different. In the following we briefly discuss the effect of probe polydispersity following the approach of Forman *et al* [22]. Within this approach we assume non-interacting probes as well as the absence of competitive hybridization reactions.

The polydispersity is specified by the fraction of probes of length i, P_i. For the case of *in situ* synthesis i denotes a probe whose growth was arrested at the ith step of the synthesis. It is however possible to produce a polydispersed probe layer by using a mixture of presynthesized probes, thus allowing one to form an arbitrary distribution of probes. The hybridization of each i probe individually follows a Langmuir isotherm where K_{it} is the equilibrium constant of the reaction $p_i + t \rightleftharpoons p_i t$. Clearly, K_{it} varies with i. Accordingly

$$x_{\mathrm{eq}}(i) = \frac{K_{it} c_t}{1 + K_{it} c_t} \tag{33}$$

while the observed overall hybridization is

$$X_{\mathrm{eq}} = \sum_{i=1}^{n} P_i x_{\mathrm{eq}}(i) = \sum \frac{P_i K_{it} c_t}{1 + K_{it} c_t}. \tag{34}$$

To illustrate the effect of probe polydispersity, consider the simplest case, of two probes of different lengths, n_1 and n_2, having equilibrium constants K_1 and K_2. The resulting

$$X_{\mathrm{eq}} = \frac{c_t(P_1 K_1 + P_2 K_2) + c_t^2 K_1 K_2}{(1 + K_1 c_t)(1 + K_2 c_t)} \tag{35}$$

deviates from the Langmuir form. *In situ* synthesis results in a truncated Poisson distribution of the probes in the range $1 \leqslant i \leqslant n$. In this case the isotherm is expected to approach the Sips isotherm [55, 56]. This generalizes the Langmuir isotherm, that allows for a single type

of adsorption site associated with a unique adsorption energy, by introducing an exponential distribution of sites with different adsorption energies, thus leading to

$$X_{\mathrm{eq}} = \left(\frac{c_t}{c_t + A}\right)^a. \tag{36}$$

Here A depends on T only and a is a constant depending on the distribution.

Altogether, caution is necessary when invoking the Langmuir isotherm in the modelling of DNA microarrays produced by *in situ* synthesis of probes. Probe polydispersity may affect the hybridization isotherm. When target fragmentation is used, the resulting polydispersity in N_t may give rise to further modifications.

8. Interactions

Our discussion thus far focused on probe layers of low surface density. In particular, it concerned systems where the distance between probe sites is large compared to the range of interaction between the probes, hybridized or not. This requirement is often unfulfilled and interactions do play a role, thus requiring modification of the Langmuir-type hybridization isotherm. In discussing the interactions and their onset it is helpful to utilize well established results from the physics of polymer brushes. To this end, note that oligonucleotide chips comprise grafted charged polymers, polyelectrolytes, terminally anchored to a planar surface. At high grafting densities the chains begin to overlap, thus forming a polyelectrolyte brush [57–59]. The discussion of polyelectrolyte brushes invokes three types of interaction: hard core repulsion between the monomers supplemented by van der Waals attraction and electrostatic repulsion. DNA chips experiments are normally carried out in high salt conditions: the hybridization solution typically contains NaCl at a concentration of $c_{\mathrm{s}} = 1$ M and the Debye length, $r_{\mathrm{D}} = 1/\sqrt{8\pi l_{\mathrm{B}} c_{\mathrm{s}}}$, is approximately 3 Å. In this 'high salt' regime the long ranged electrostatic repulsion is screened and the behaviour of the brush is dominated by excluded volume interactions. Consequently the onset of interactions occurs when the tethered chains begin to overlap. To delineate the interaction regimes it is first necessary to specify the dimensions of the hybridized and non-hybridized probes in the low grafting density limit.

To implement the polymer physics description of the probe layer it is helpful to begin with the second virial coefficient of monomer–monomer interactions, v. In the high salt regime v comprises two terms [40]:

$$v = \frac{2\pi}{3}a^3\left(1 - \frac{\theta}{T}\right) + 2\pi l_{\mathrm{B}} r_{\mathrm{D}}^2. \tag{37}$$

The first allows for the hard core repulsion between spherical monomers of radius a as modulated by a weak van der Waals attraction giving rise to the $(1 - \theta/T)$ factor. Here θ is the theta temperature where monomer–monomer interactions between neutral monomers vanish. The second term reflects the screened electrostatic interactions between the monomers where $l_{\mathrm{B}} = e^2/\epsilon kT \approx 7$ Å is the Bjerrum length and ϵ is the temperature dependent dielectric constant of water [60]. The value of θ of ssDNA remains to be established. Additionally v as given by (37) does not allow for hydrogen bonding, water structure, the role of stacking interactions between the monomers and for the possible contribution of electrostatic correlations. With these reservations we will use (37) to obtain the interaction free energies. For consistency, we will also use this v to estimate the dimensions of the ssDNA probes.

The dimensions of dsDNA in the relevant range of n and N_t are well established [61]. In this range dsDNA is a rod-like, cylindrical molecule with each base pair contributing $b = 3.4$ Å to its length. The radius of dsDNA is 9.5 Å and its cross sectional area is thus 284 Å^2. The

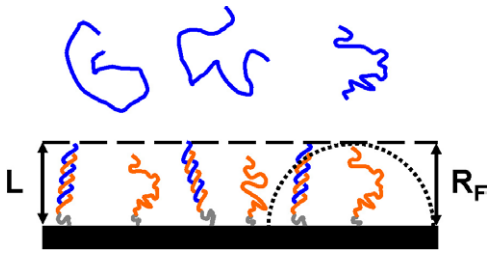

Figure 8. A mixed brush of ds and ss DNA chains is formed upon hybridization of high density DNA chips with oligonucleotide targets, $N_t = n$.

situation is less clear with regard to ssDNA which behaves as a semiflexible chain. Its swelling behaviour requires knowledge of its monomer size whose value, as cited in the literature, is $a = 6$ Å [62, 63]. With this value of a the second term in v is comparable to a^3, thus suggesting athermal solvent behaviour. In turn, this implies that ssDNA chains comprising N bases attain their Flory radius, $R_F \sim N^{3/5}a$, for all N. Since ssDNA is actually a semiflexible chain characterized by a persistence length l_p the Flory radius is $R_F \approx (Na/l_p)^{3/5}l_p$ where l_p/a is the number of monomers in a persistent segment. The estimation of R_F of ssDNA is however hampered by an uncertainty regarding l_p. The reported values vary over a wide interval in the range 7.5 Å $\leqslant l_p \leqslant$ 35 Å [50]. Note further that while the role of excluded volume interaction has been recognized, the span of ssDNA is often estimated by the ideal coil dimension $R_0 \approx (Na/l_p)^{1/2}l_p$. With these caveats, one may use the lower bound $R_F \approx N^{3/5}a$ as a rough estimate of the span of ssDNA. This background enables us to discuss the onset of interactions and the associated modification of the hybridization isotherms. To this end it is helpful to consider two scenarios: in physical chemistry and calibration experiments the targets are often oligonucleotides with $N_t = n$. In contrast, in biology experiments the targets are typically much longer, $N_t \gg n$. We first consider the $N_t = n$ case and then elaborate the discussion to describe the long targets scenario.

The inherent difficulty in describing the $N_t = n$ case is due to the formation of a mixed, two-component brush comprising hybridized (pt) and non-hybridized (p) probes (figure 8). Allowing for short flexible spacers, we view the hybridized probes as rigid rods, of length $L = nb$, freely jointed to the surface. The unhybridized probes behave as semiflexible coils whose span is the Flory radius $r_F \approx (na/l_p)^{3/5}l_p$. In general $r_F \neq L$. Two difficulties now occur. One concerns the identification of the overlap threshold. It arises because the interaction range is different for the three possible neighbouring probe sites $p \leftrightarrow p$, $p \leftrightarrow pt$ and $pt \leftrightarrow pt$. A related difficulty also hampers the analysis of the brush regime. In the strong overlap regime the brush consists of a mixture of ds pt and ss p, of different configurations and dimensions. A general description requires the introduction of three different virial coefficients corresponding to the three possible interactions $p \leftrightarrow p$, $p \leftrightarrow pt$ and $pt \leftrightarrow pt$. Furthermore, it is necessary to distinguish between brushes obtained for $r_F > L$ and $r_F < L$. In both cases, the simplest brush model should distinguish between two regions: an inner layer populated by both species and an outer layer containing only the species whose free ends attain the highest altitude.

These difficulties can be circumvented when n is sufficiently small. In particular, since $b = 3.4$ Å while 7.5 Å $\leqslant l_p \leqslant$ 35 Å there is a range of n where $r_F \approx L$. This range is determined by the condition $na/l_p \approx (a/b)^{5/2} \approx 4$. For a reasonable estimate of l_p it is fulfilled for short probes in the experimentally relevant range. For example, choosing 10 Å $\leqslant l_p \leqslant$ 15 Å one obtains $12 \leqslant n \leqslant 18$. Our discussion for $N_t = n$ will thus focus on this range. We can now distinguish between two regimes. When $\Sigma_0 > r_F^2$ there are no interactions between the

probes, irrespective of their hybridization state, and a Langmuir-type isotherm is expected. In the opposite case, of $\Sigma_0 < r_F^2$, interactions do play a role: a brush is formed, thus requiring a modification of the Langmuir behaviour. As noted before, a general model of a mixed brush of ssDNA and dsDNA is difficult to formulate. This difficulty persists in the range of n considered here. However, we can obtain the leading behaviour by using two rough approximations: first, we assume that the layer thickness is roughly L, irrespective of the hybridization fraction, x. This is clearly the case in the weak overlap regime when the crowding induced stretching of the ssDNA is small. At smaller Σ_0 this assumption is justified because the extension of ssDNA favours stacking interactions and thus the formation of a single-stranded helix with $b = 3.4$ Å [51, 52]. Second, we will estimate the interaction energy in the brush regime as the corresponding Flory free energy. The interaction free energy density of the probe layer is thus $G_{\rm int}/L\Sigma_0 = kTvc^2$ where $c = n(1+x)/\Sigma_0 L$ is the number concentration of monomers within the layer. In our approximation scheme each ds pt probe contributes $n + N_t = 2n$ monomers while a ss p chain contributes n. Within this scheme there is no distinction between bases belonging to ds and ss DNA. Accordingly, a single v is involved. On the basis of (37), we estimate $v \approx 2\pi l_B r_D^2$, thus obtaining a free energy per site

$$\frac{G_{\rm int}}{kT} = 2\pi l_B r_D^2 \frac{n^2(1+x)^2}{\Sigma_0 L}. \tag{38}$$

In view of the rough approximations invoked it is pointless to incorporate the relatively weak effects due to the impenetrable wall. Accordingly, the equilibrium condition $\mu_t = \mu_{pt}^{\rm ex} = \partial\gamma_{\rm site}/\partial x$ yields

$$\frac{x_{\rm eq}}{1-x_{\rm eq}} = c_t K_{pt} \exp\left[-\Gamma(1+x_{\rm eq})\right] \tag{39}$$

with $\Gamma = 4\pi n^2 l_B r_D^2/\Sigma_0 L$. The main conclusion from (39) is that the hybridization in the brush regime becomes more difficult as the hybridization degree grows because of the penalty incurred upon introducing the targets into the probe layer. We now turn to alternative approaches leading to this result in order to clarify the underlying physics.

The discussion presented above utilized the Flory free energy when the virial coefficient of monomer–monomer interactions was dominated by screened electrostatic interactions between the charged monomers. It is instructive to compare this to derivations focusing on the electrostatic free energy. Of these, the simplest is that based on the capacitor model for interfacial double layers. In it, all charges due to the DNA are distributed in an infinitely thin layer at the solid–liquid interface. The charged surface together with a diffuse neutralizing layer of counterions form a double layer of width r_D. In the high salt regime $G_{\rm int}(x)/\Sigma_0$ may thus be identified with the electrostatic energy per unit area of a planar capacitor, $2\pi(\sigma e)^2 d/\epsilon$, of width $d \approx r_D$. Here $\sigma = \sigma_0(1+x)$ is the number charge density and $\sigma_0 = n/\Sigma_0$ is its initial value corresponding to an unhybridized probe layer. Altogether,

$$\frac{G_{\rm int}(x)}{kT} = 2\pi\sigma^2 l_B r_D \Sigma_0 = 2\pi l_B r_D \frac{n^2(1+x)^2}{\Sigma_0} \tag{40}$$

and the resulting hybridization isotherm has an identical form to (39) but Γ is replaced by a larger $\Gamma_c = 4\pi n^2 l_B r_D/\Sigma_0 = L\Gamma/r_D$. The difference between Γ and Γ_c is due to the localization of the charges at the solid–liquid interface leading to an overestimate of the electrostatic interactions. To correct this overestimate one may smear the charges in a layer of thickness L. This can be achieved using the box approximation for the solution of the Poisson–Boltzmann equation leading, up to a factor of 2, to the results obtained from the brush model [38]. The box model also allows one to analyse the hybridization behaviour in solutions of lower ionic strength where the hybridization isotherm assumes a qualitatively different form.

A different model addressing the effects of electrostatic interactions on the hybridization isotherms was proposed in a series of pioneering articles by Vainrub and Pettitt (VP) [32–36]. It yields a hybridization isotherm of the form (39) but with somewhat different Γ. The VP approach is designed so as to utilize exact results, obtained by Ohshima and Kondo [64], on the interaction free energy between a penetrable charged sphere and an impenetrable charged surface in the strong screening regime when the Debye–Hückel approximation is applicable. Within it, one calculates the excess free energy of a probe layer incorporating xN_{T} hybridized probes, $G_{\mathrm{el}}(x)$, with respect to an unhybridized layer comprising N_{T} probes. In effect, $G_{\mathrm{el}}(x)$ is the sum of the contributions of xN_{T} hybridization events, $G_{\mathrm{el}} = \sum_{i=1}^{xN_{\mathrm{T}}} G_i(\sigma_i)$, each occurring at a different charge density $\sigma_i = \sigma_0 + \mathrm{i}n/A$ where A is the surface area of the spot. At each step the probe layer is modelled as a planar charged surface interacting with a *single* charged sphere. The ith hybridization step experiences a charge density σ_i reflecting uniform smearing of the charges of all other probes, hybridized or unhybridized. In the VP model, the associated free energy term is $G_i(\sigma_i) = G_{pt}(\sigma_i) - G_p(\sigma_i)$ where $G_{pt}(G_p)$ is the electrostatic free energy of a $pt\,(p)$ sphere in contact with a planar layer with charge density σ_i. The VP approach relies on a prescription for assigning an effective sphere to the p (pt) chains. It cannot be extended to describe the hybridization at lower ionic strength when the Ohshima and Kondo result does not apply. More important, its extension to the $N_t \gg n$ case, when the thickness of the probe layer changes with x, is difficult.

The four models describing the $N_t = n$ case at the high salt all lead to an isotherm of the form

$$\frac{x_{\mathrm{eq}}}{1 - x_{\mathrm{eq}}} = c_t K_{pt} \exp\left[-\mathrm{const}(1 + x_{\mathrm{eq}})\right]. \tag{41}$$

In terms of equation (6) it corresponds to $f(x_{\mathrm{eq}}) = \exp[-\mathrm{const}(1 + x_{\mathrm{eq}})]$. This form reflects two ingredients.

(i) The number of monomers in the probe layer grows with the hybridization. This is inseparable from the increase of positive charge localized in the probe layer.
(ii) The thickness of the layer remains constant.

Hybridization leads thus to an increase of the monomer concentration within a layer of *constant* thickness and a consequent increase in the monomer–monomer interactions. Of the models discussed, the brush model affords two advantages: simplicity as well as a built-in criterion for the onset of the interactions. In addition it is straightforward to apply this model to biological-type experiments where $N_t \gg n$ and the constant thickness assumption fails. The box model is advantageous in that it enables the analysis of the low salt case where the simple brush model, as described above, does not work.

In biology experiments using oligonucleotide arrays, the targets are much longer than the probes, $N_t \gg n$. As a result, the hybridized probes carry long tails of ssDNA (figure 9). These tails, which are absent when $N_t = n$, are the origin of the differences between the two situations [40]. The distinctive aspects of the 'long tails' scenario are first apparent in the interaction regimes which reflect two length scales. As before, an isolated unhybridized probe, p, occupies a hemisphere of radius $r_{\mathrm{F}} \sim n^{3/5}a$. The configurations of the pt pair depend on the position of the hybridization site with the target. When it is situated within the target, the pt will carry two tails. For brevity we consider the simplest case, that of a hybridization site at the end of the target when a pt carries a single ssDNA tail comprising $N_t - n$ unhybridized bases. For oligonucleotide probes, the overall span of the pt is dominated by the monomer cloud formed by the tail and the contribution of the hybridized ds probe is negligible. This span is characterized by the Flory radius $R_{\mathrm{F}} \sim (N_t - n)^{3/5}a \approx N_t^{3/5}a$. The unhybridized probes do not interact when $r_{\mathrm{F}}^2 < \Sigma_0$. Similarly, when $R_{\mathrm{F}}^2 < \Sigma_0$ there is no interaction between

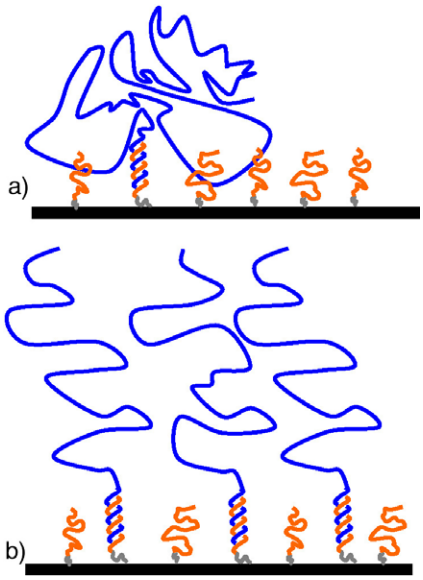

Figure 9. When $N_t \gg n$ hybridization results in probes carrying a long ssDNA tail. In the case of $R_F^2 \gg \Sigma_0$ two regimes occur: (a) a mushroom regime when the tails do not crowd each other and (b) a brush regime that develops past the overlap threshold.

the hybridized probes and consequently no brush regime. It is thus possible to distinguish between three different scenarios. A Langmuir isotherm is expected when $\Sigma_0 > R_F^2 > r_F^2$. Brush effects, due to the crowding of the hybridized probes but with no interactions between the probes, will occur when $r_F^2 < \Sigma_0 < R_F^2$ (figure 9). Finally, when $\Sigma_0 < r_F^2 < R_F^2$, both brush effects and probe–probe interactions play a role. All three scenarios occur in the reported variety of DNA chip experiments.

In the following we will discuss the $r_F^2 < \Sigma_0 < R_F^2$ case, when the interactions between the ss probes do not contribute. As in the $N_t = n$ case, the surface layer consists of a binary mixture of p and pt of different configurations and dimensions. The $N_t \gg n$ case is however different in two respects. First, the dominant free energy term is due to the overlap between the ssDNA tails. In marked distinction from the situation encountered for $N_t = n$, the interaction between ssDNA and dsDNA is relatively small, thus simplifying the analysis. On the other hand, the $r_F^2 < \Sigma_0 < R_F^2$ condition implies that the tails also interact with neighbouring unhybridized probes. Thus, at low x values, when there are no tail–tail interactions, it is still necessary to allow for the interactions between a tail and R_F^2/Σ_0 unhybridized p chains. A detailed analysis, allowing for this effect as well as the impenetrable wall, was presented in [40]. In the following we limit the discussion to the leading correction to the hybridization isotherm, due to the formation of a brush of long tails:

$$\frac{x_{eq}}{1 - x_{eq}} \simeq c_t K_{pt} \exp\left[-N_t (x_{eq}^{2/3} - x_B^{2/3}) \left(\frac{a^2}{\Sigma_0}\right)^{2/3}\right]. \tag{42}$$

In this case, $f(x_{eq})$ as defined in (6) assumes the form $f(x_{eq}) \sim \exp[-\text{const}'(x_{eq}^{2/3} - x_B^{2/3})]$. This reflects the free energy per probe in a brush with an area per hybridized probe $\Sigma = \Sigma_0/x$:

$$\frac{G_{int}}{RT} \simeq N_t \left(\frac{a^2}{\Sigma_0}\right)^{2/3} x^{5/3}. \tag{43}$$

Equation (42) differs from (41) in two aspects of the exponential factor: first, the exponent in (41) contains $(1 + x_{eq})$ because the interactions involve both p and pt chains. In contrast, only the interactions between tail carrying pt chains contribute to (42). Second, the exponent in (41) is linear in x_{eq} while in (42) it varies with $x_{eq}^{2/3}$. This is because the height of a brush of flexible chains varies with $\Sigma \sim 1/x_{eq}$, in contrast to the $N_t = n$ case where our discussion suggested a constant brush thickness. In the $N_t \gg n$ case the long tails stretch out along the normal to the surface so as to lower the monomer concentration and the associated monomer–monomer interactions. While $f(x_{eq})$ in both (41) and (42) assumes an exponential form, this is not always the case. In solutions of lower ionic strength, $f(x_{eq})$ may exhibit a power law dependence on x_{eq} [38].

9. A little on Latin square experiments

A detailed discussion of the theoretical analysis [27–29, 65–69] of Latin square experiments [16] is beyond the scope of this review. This topic is considered in depth in the articles of Binder [70] and of Carlon and Heim [71] in this issue. Here we only comment on the relationship between our earlier discussion and a significant result that emerged from the analysis of these experiments, in particular, the possibility of fitting the plots of spot intensities versus spike concentration utilizing the Langmuir form and an effective temperature, T_{eff}, used as an adjustable parameter. In these fits $\Delta G^0_{pt}(T_h)$ of the hybridization reaction is obtained from the NN model for the hybridization temperature, T_h, and the equilibrium constant is thus $K_{pt} = \exp[-\Delta G^0_{pt}(T_h)/RT_{eff}]$. $T_{eff} \approx 2000$ K is found when $\Delta G^0_{pt}(T_h)$ is calculated for DNA–DNA ds [28]. It is reduced to $T_{eff} \approx 700$ K when $\Delta G^0_{pt}(T_h)$ corresponds to DNA–RNA ds [69]. The fitting procedures used in the two articles are different but both find $T_{eff} > T_h$. Upon writing $K_{pt} = \exp[-\alpha \Delta G^0_{pt}(T_h)/RT_h]$ with $\alpha = T_h/T_{eff} < 1$, this indicates a reduction of the hybridization free energy at the surface from ΔG^0_{pt} to $\alpha \Delta G^0_{pt}$. The physical origins of this reduction are not yet established. One contributing factor is the presence of dimethyl sulfoxide (DMSO), a denaturant [72, 73], in the hybridization solution [74]. It is however difficult to quantify the associated effects because the dependence of the NN free energies on the DMSO concentration is not available at present. Within the framework of our earlier discussion, three additional candidates come to mind. Held *et al* [28] as well as Carlon and Heim [69] point out the possible role of competitive bulk hybridization. As discussed earlier, the Langmuir form is retained but with a reduced equilibrium constant $\approx K_{pt}/K_h$ when hairpin formation is the only competitive hybridization reaction and there are no interactions. The role of this mechanism is likely to be diminished by the DMSO. It is of interest to note the possible role of two supplementary factors. First, interactions within the probe layer can also contribute to the reduction of the effective ΔG^0_{pt}. Since the interactions penalize hybridization, the corresponding isotherm lies below the interaction free Langmuir isotherm. As a result, fitting the 'interaction isotherm' using a Langmuir form will yield $T_{eff} > T_h$ (figure 10). To illustrate this point, we present the T_{eff} values as obtained from fitting calculated $x_{eq}(c_t)$ allowing for brush effects [40] to the Langmuir form (figure 11). The results depicted here were obtained for the non-fragmented target in a denaturant free solution. Fragmentation will diminish the brush effect while the denaturant will enhance it. Estimation of the overall effect is currently impossible because the N_t distribution following fragmentation is unknown and due to the lack of full data concerning the effects of DMSO. Failure to attain equilibrium can also contribute to the occurrence of $T_{eff} > T_h$. In such a case the observed $x = x(c_t)$ curve lies below the hybridization isotherm, thus leading to $T_{eff} > T_h$. For a denaturant free system this is a significant factor. This is evident from the fastest kinetics of hybridization in reaction

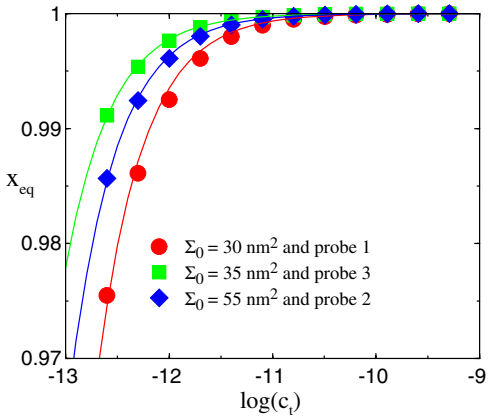

Figure 10. The hybridization isotherm of three out of the sixteen probes of gene 37777_at with perfectly matched targets spiked in, at concentrations $c_t = 0.5, 1, 2, 4, 8, 16, 32, 64, 128, 256, 512$ and 1024 pM for different Σ_0. The hybridization temperature is $T_h = 45\,^{\circ}\mathrm{C}$ and the target comprises $N_t = 328$ bases (prefragmentation value). The corresponding ΔG^0_{pt} are specified by the NN method for DNA–RNA [43–46]. The calculated x_{eq}, allowing for brush effects [40], are fitted to a Langmuir isotherm, thus determining T_{eff} (figure 11).

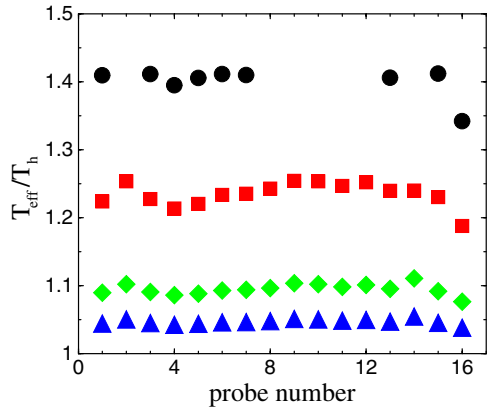

Figure 11. T_{eff}/T_h for the sixteen probes of gene 37777_at, as obtained from fits such as that depicted in figure 10 for $\Sigma_0 = 30$ nm^2 (circles), 50 nm^2 (squares), 100 nm^2 (diamonds) and 150 nm^2 (triangles).

controlled systems free of interactions or competition. The Langmuir kinetics describing this situation are specified by $\mathrm{d}x/\mathrm{d}t = k_h(1-x)c_t - k_d x$ where k_h and k_d are the hybridization and denaturation rate constants at the surface. The time dependent hybridization fraction is thus $x(t) = x_{eq}[1-\exp(-t/\tau)]$ where $\tau^{-1} = k_d + k_h c_t$. When seeking an order of magnitude estimate it is permissible to ignore the surface corrections to the rate constants and to utilize their approximate bulk values $k_h \simeq 10^6\ \mathrm{M}^{-1}\ \mathrm{s}^{-1}$ and $k_d = k_h/K^0_{pt} = k_h \exp[\Delta G^0_{pt}/RT]$ [51]. For c_t in the 10^{-12}–10^{-9} M range, $n = 25$ and a denaturant free solution, $k_d \ll k_h c_t$ leading to $\tau \simeq 1/k_h c_t \simeq 10^6$–$10^9$ s. The hybridization in the Affymetrix protocol is $t_h = 16\,\mathrm{h} \simeq 6\times10^4$ s and $\tau \gg t_h$, thus indicating incomplete equilibration. Importantly the presence of DMSO should lower $|\Delta G^0_{pt}|$ and may well modify k_h, so smaller τ values are possible. Accordingly the preceding argument cannot be used to evaluate the degree of hybridization and its contribution

to $T_{\mathrm{eff}} > T_{\mathrm{h}}$. It only serves to draw attention to this issue. Altogether, our discussion suggests that the analysis of Latin square experiments can benefit from additional information about the effects of DMSO on the kinetics and equilibrium behaviour, the distribution of N_t resulting from the fragmentation step and the values of the area per probe, Σ_0.

10. On the development of the theory of DNA chips

Our presentation thus far aimed at a unified picture of hybridization isotherms of DNA chips. At this point we briefly comment on the different contributions to the development of the theory in this domain, focusing as announced on the 'physical chemistry' direction. The pioneering theory papers on the function of DNA chips dealt with the role of target diffusion, assuming that the equilibrium behaviour is described by a Langmuir isotherm with the bulk values of K and the rate constants. The work of Livshits and Mirzabekov focused on the diffusion into DNA chips with probes bound into thin pads of water-soluble gels [31]. Chan *et al* considered DNA chips with probes attached to impenetrable surfaces allowing for the role of lateral, two-dimensional diffusion of physisorbed targets [30]. These two articles considered the case of a given spot contacted with a solution containing a single target. The effect of competitive surface hybridization was first analysed in a numerical study by Bhanot *et al* who investigated the development of hybridization at a number of spots contacted with a multicomponent solution of targets with no bulk hybridization [37]. Importantly, this demonstrated that the performance of the chip is best when equilibrium is attained. Forman *et al* analysed the effect of probe polydispersity resulting from *in situ* synthesis on the observable hybridization behaviour [22]. The role of electrostatic interaction within the probe layer was first considered in a series of papers by Vainrub and Pettitt [32–36]. Hagan and Chakraborty discussed the initial hybridization rate constants when the unhybridized probes form a brush [75]. The effect of bulky fluorescent labels on the hybridization was first considered theoretically by Naef and Magnasco [42].

11. Discussion

Our discussion focused on the equilibrium behaviour of DNA chips as characterized by their hybridization isotherms. This choice is motivated by three observations concerning hybridization isotherms as guides to design and interpretation of DNA chip experiments. The most fundamental is that hybridization isotherms determine the upper bound of the performance of DNA chips, a point first stressed by Bhanot *et al* [37]. This feature is traceable to the characteristics of the hybridization rate constants. The hybridization process is thought to involve a nucleation rate controlling step. As a result, the hybridization constants are very similar, exhibiting a weak sequence dependence. In contrast, the denaturation rate constant is strongly dependent on n and the sequence. This is because the corresponding activation step requires break-up of all base pairs short of the nucleation site [51]. As a result, the initial hybridization of a DNA chip contacted with a multicomponent solution will reflect significant fraction of mishybridization events. The fraction of mishybridized probes decreases with time as the probes equilibrate by a series of denaturation and rehybridization steps. The performance of the device should thus improve as equilibrium is approached. This discussion leads us to the second observation. The hybridization isotherms are simple in comparison to the kinetics schemes that govern hybridization at the surface. Issues of diffusion versus reaction control are avoided and the number of pertinent parameters is much smaller. Finally, a clear understanding of the equilibrium state is necessary for the analysis of the kinetics. These three observations

justify our focus on hybridization isotherms that already provide, explicitly or implicitly, the theoretical foundation for the design of DNA chips and the analysis of their results.

There is however a striking contrast between the experimental status of hybridization isotherms and their central role in the modelling, design and analysis of DNA chips. The number of reported hybridization isotherms is very small. In turn, this is related to experimental difficulties. To establish the minimal requirements of thermodynamic equilibrium it is necessary to reach a stationary, time independent, hybridization degree $x_{\rm eq}$. Thus, the hybridization must be carried out over long periods. Experimentally observed equilibration timescales are in the range of one to two days. Checking for possible hysteresis effects, by subjecting the samples to heating and cooling cycles, makes the experimental task even more time-consuming. One additional difficulty merits comment. To obtain hybridization isotherms it is necessary to establish the number of probes available to hybridization. This also specifies Σ_0, thus allowing us to establish the role of interactions. With these difficulties in mind, it is of interest to mention a number of key experiments that have not yet been performed. They concern the determination of the hybridization isotherms for a number of simple situations. With regard to the role of competitive hybridization in the absence of interactions it is useful to study:

(i) the hybridization when the solution contains single-species ds targets with $N_t = n$ so as to establish the effect of intermolecular competitive bulk hybridization; and

(ii) the hybridization with a binary solution of two different ss targets, $N_t = n$, both capable of hybridization with the probes, in order to establish the signatures of competitive surface hybridization.

To understand the role of interactions it is necessary to experimentally study the hybridization isotherms of a series of single-component solutions of long targets. Ideally such experiments should involve systematic variation of N_t subject to two requirements: $N_t \gg n$ and $R_{\rm F}^2 \gg \Sigma_0$. In this case, it is of interest to supplement the hybridization experiments with characterization of the concentration profile of the brush using, for example, neutron reflectometry. In the opposite regime, of $R_{\rm F}^2 \ll \Sigma_0$, these experiments should shed light on the effect of the impenetrable surface on the hybridization constant at the surface. Systematic experimental studies of these 'physical chemistry' questions will help provide a solid foundation for the design and interpretation of DNA chip experiments.

List of principal symbols and abbreviations

x	the hybridization fraction
$x_{\rm eq}$	the hybridization fraction at equilibrium
c_t	the target concentration
n	the number of bases in a probe
N_t	the number of bases in a target
Σ_0	the area per probe
K_{pt}	the equilibrium constant for the probe–target hybridization at the surface
K_{pt}^0	the equilibrium constant for the probe–target hybridization as obtained from the NN method

c_{50}	the target concentration leading to $x_{eq} = 1/2$
c_{50}^0	the target concentration leading to $x_{eq} = 1/2$ as calculated from the NN method
T_m	the melting temperature of ds nucleic acid
R_F	the Flory radius
a	the monomer size of single-stranded DNA
l_p	the persistence length of single-stranded DNA
b	the projected length of a base pair along the axis of double-stranded DNA
NN	nearest neighbour method for calculating the thermodynamics of hybridization
NA	nucleic acid
PCR	polymerase chain reaction
ss	single stranded
ds	double stranded

References

[1] Graves D J 1999 *Trends Biotechnol.* **17** 127
[2] Southern E, Mir K and Shchepinov M 1999 *Nat. Genet.* **21** 5
[3] Wang J 2000 *Nucleic Acids Res.* **28** 3011
[4] Lockhart D J and Winzeler E A 2000 *Nature* **405** 827
[5] Heller M J 2002 *Annu. Rev. Biomed. End* **4** 129
[6] Pirrung M C 2002 *Angew. Chem. Int. Edn* **41** 1277
[7] Collins F S, Morgan M and Patrinos A 2003 *Science* **300** 286
[8] Rouse R and Hardiman G 2003 *Pharmacogenomics* **4** 623
[9] Gabig M and Wegrzyn G 2001 *Acta Biochim. Pol.* **48** 615
[10] Levicky R and Horgan A 2005 *Trends Biotechnol.* **23** 143
[11] Brazma A *et al* 2001 *Nat. Genet.* **29** 365
[12] Gabor Miklos G L and Maleszka R 2004 *Nat. Biotechnol.* **22** 615
[13] Tan P K *et al* 2003 *Nucleic Acids Res.* **31** 5676
[14] Yauk C L, Berndt M L, Williams A and Doublas G R 2004 *Nucleic Acids Res.* **32** e124
[15] Lodish H 2000 *Molecular Cell Biology* (New York: Freeman)
[16] Affymetrix. Latin Square Data for Expression Algorithm Assessment.
WebSite: http://www.affymetrix.com/support/technical/sample_data/datasets.affx
[17] Guo Z, Guilfoyle R A, Thiel A J, Wang R and Smith L M 1994 *Nucleic Acids Res.* **22** 5456
[18] Georgiadis R, Peterlinz K P and Peterson A W 2000 *J. Am. Chem. Soc.* **122** 3166
[19] Nelson B P, Grimsrud T E, Liles M R, Goodman R M and Corn R M 2001 *Anal. Chem.* **73** 1
[20] Peterson A W, Wolf L K and Georgiadis R M 2002 *J. Am. Chem. Soc.* **124** 14601
[21] Su H-J, Surrey S, McKenzie S E, Fortina P and Graves D J 2002 *Electrophoresis* **23** 1551
[22] Forman J E, Walton I D, Stern D, Rava R P and Trulson M O 1998 *ACS Symp. Ser.* **682** 206
[23] Okahata Y, Kawase M, Niikura K, Ohtake F, Furusawa H and Ebara Y 1998 *Anal. Chem.* **70** 1288
[24] Steel A B, Herne T M and Tarlov M J 1998 *Anal. Chem.* **70** 4670
[25] Dai H, Meyer M, Stepaniants S, Ziman M and Soughton R 2002 *Nucleic Acids Res.* **30** e86
[26] Kepler T B, Crosby L and Morgan K T 2002 *Genome Biol.* **3** 0037
[27] Hekstra D, Taussig A R, Magnasco M and Naef F 2003 *Nucleic Acids Res.* **31** 1962
[28] Held G A, Grinstein G and Tu Y 2003 *Proc. Natl Acad. Sci. USA* **100** 7575
[29] Zhang L, Miles M F and Aldape K D 2003 *Nat. Biotechnol.* **21** 818
[30] Chan V, Graves D J and McKenzie S 1995 *Biophys. J.* **69** 2243
[31] Livshits M A and Mirzabekov A D 1996 *Biophys. J.* **71** 2795
[32] Vainrub A and Pettitt M B 2000 *Chem. Phys. Lett.* **323** 160
[33] Vainrub A and Pettitt M B 2002 *Phys. Rev.* E **66** 041905
[34] Vainrub A and Pettitt M B 2003 *J. Am. Chem. Soc.* **125** 7798
[35] Vainrub A and Pettitt M B 2003 *Biopolymers* **68** 265
[36] Vainrub A and Pettitt M B 2004 *Biopolymers* **73** 614
[37] Bhanot G, Louzoun Y, Zhu J and DeLisi C 2003 *Biophys. J.* **84** 124
[38] Halperin A, Buhot A and Zhulina E B 2004 *Biophys. J.* **86** 718
[39] Halperin A, Buhot A and Zhulina E B 2004 *Clin. Chem.* **50** 2254

[40] Halperin A, Buhot A and Zhulina E B 2005 *Biophys. J.* **89** 796
[41] Stekel D 2003 *Microarray Bioinformatics* (Cambridge: Cambridge University Press)
[42] Naef F and Magnasco M 2003 *Phys. Rev.* E **68** 011906
[43] SantaLucia J 1998 *Proc. Natl Acad. Sci. USA* **95** 1460
[44] SantaLucia J and Hicks D 2004 *Annu. Rev. Biophys. Biomol. Struct.* **33** 415
[45] Peyret N, Seneviratne P A, Allawi H T and SantaLucia J 1999 *Biochemistry* **38** 3468
[46] HyTher^{TM} Version 1.0 Peyret N and SantaLucia J Wayne State University. Web site: http://ozone2.chem.wayne.edu/
[47] Fotin A V, Drobyshev A L, Proudnikov D Y, Perov A N and Mirzabekov A D 1998 *Nucleic Acids Res.* **26** 1515
[48] Duplantier B 1989 *J. Stat. Phys.* **54** 581
[49] Eisenriegler E, Kremer K and Binder K 1982 *J. Chem. Phys.* **77** 6296
[50] Mills J B, Vacano E and Hagerman P J 1999 *J. Mol. Biol.* **285** 245
[51] Turner D H, in Bloomfield V A, Crothers D and Tinoco I Jr 2000 *Nucleic Acids: Structures, Properties and Functions* (Sausalito: University Science Books)
[52] Buhot A and Halperin A 2004 *Phys. Rev.* E **70** 020902(R)
[53] Kirk B W, Feinsod M, Favis R, Kliman R M and Barany F 2002 *Nucleic Acids Res.* **30** 3295
[54] Prix L, Uciechowski P, Böckmann B, Giesing M and Schuetz A J 2002 *Clin. Chem.* **48** 428
[55] Sips R 1948 *J. Chem. Phys.* **16** 490
[56] Sips R 1950 *J. Chem. Phys.* **18** 1024
[57] Milner S T 1991 *Science* **251** 905
[58] Halperin A, Tirrell M and Lodge T P 1992 *Adv. Polym. Sci.* **100** 31
[59] Rühe J *et al* 2004 *Adv. Polym. Sci.* **165** 77
[60] Evans D F and Wennerström H 1994 *The Colloid Domain* (New York: VHC)
[61] Cantor C R and Schimmel P R 1980 *Biophysical Chemistry* (New York: Freeman)
[62] Smith S B, Cui Y J and Bustamante C 1996 *Science* **271** 795
[63] Strick T R, Dessinges M-N, Charvin G, Dekker N H, Allemand J-F, Bensimon D and Croquette V 2003 *Rep. Prog. Phys.* **66** 1
[64] Ohshima H and Kondo T 1993 *J. Colloid Interface Sci.* **157** 504
[65] Binder H, Kirsten T, Loeffler M and Stadler P F 2004 *J. Phys. Chem.* B **108** 18003
[66] Binder H, Kirsten T, Hofacker I L, Stadler P F and Loeffler M 2004 *J. Chem. Phys.* B **108** 18015
[67] Binder H and Preibisch S 2005 *Biophys. J.* **89** 337
[68] Burden C J, Pittelkow Y and Wilson S R 2005 *Preprint* q-bio.BM/0411005
[69] Carlon E and Heim T 2005 *Preprint* q-bio.BM/0411011
[70] Binder H 2006 *J. Phys.: Condens. Matter* **18** S491
[71] Heim T *et al* 2006 *J. Phys.: Condens. Matter* **18** S525
[72] Strauss J H, Kelly R B and Sinsheimer R L 1968 *Biopolymers* **6** 793
[73] Kotler L, He H, Miller A W and Karger B L 2002 *Electrophoresis* **23** 3062
[74] Affymetrix GeneChip Expression Analysis Technical Manual. Section 2: Eukaryotic Sample and Array Processing and Section 3: Prokaryotic Sample and Array Processing.
[75] Hagan M F and Chakraborty A K 2004 *J. Chem. Phys.* **120** 4958